15th ASCE Engineering Mechanics Conference
June 2-5, 2002, Columbia University, New York, NY

APPLICATION OF SUBSET SIMULATION TO SEISMIC RISK ANALYSIS

Siu-Kui Au [1], Associate Member, ASCE,
and James L. Beck[2], Member, ASCE

ABSTRACT

This paper presents the application of a new reliability method called Subset Simulation to seismic risk analysis of a structure, where the exceedance of some performance quantity, such as the peak interstory drift, above a specified threshold level is considered for the case of uncertain seismic excitation. This involves analyzing the well-known but difficult first-passage failure problem. Failure analysis is also carried out using results from Subset Simulation which yields information about the probable scenarios that may occur in case of failure. The results show that for given magnitude and epicentral distance (which are related to the 'intensity' of shaking), the probable mode of failure is due to a 'resonance effect.' On the other hand, when the magnitude and epicentral distance are considered to be uncertain, the probable failure mode corresponds to the occurrence of 'large-magnitude, small epicentral distance' earthquakes.

Keywords: First passage problem, Markov Chain Monte Carlo simulation, reliability, Subset Simulation, seismic risk

INTRODUCTION

Structural reliability is concerned with the probability that a structure will not reach some specified state of failure in some uncertain environment. Let $\underline{\theta} = [\theta_1, \ldots, \theta_n] \in \mathbb{R}^n$ be a parameter vector containing all the uncertain quantities of interest; in general, they can relate to the structural behavior and the loading conditions. Let $q : \mathbb{R}^n \mapsto [0, \infty)$ be a prescribed probability density function (PDF) quantifying the relative plausibility of values that the set of uncertain parameters $\underline{\theta}$ may assume. The failure probability can be formulated as

$$P(F) = \int \mathbb{I}_F(\underline{\theta})\, q(\underline{\theta})\, d\underline{\theta} \tag{1}$$

where $F \subset \mathbb{R}^n$ denotes the failure region and $\mathbb{I}_F : \mathbb{R}^n \mapsto \{0, 1\}$ is the indicator function: $\mathbb{I}_F(\underline{\theta}) = 1$ if $\underline{\theta} \in F$ and $\mathbb{I}_F(\underline{\theta}) = 0$ otherwise. Much attention has been given to the evaluation of the failure probability in the past few decades (e.g., Engelund and Rackwitz 1993; Schuëller et al. 1993), which constitutes the domain of reliability methods. To date, efficient methods exist for solving time-independent (static) reliability problems where the number of uncertain parameters is not too large. However, efficient and robust simulation methods for solving general time-dependent (dynamic) reliability problems are still at their early exploration stage (Schuëller et al. 1993).

[1] School of Civil and Environmental Engineering, Nanyang Technological University, Singapore 639798, Singapore. E-mail: cskau@ntu.edu.sg

[2] Division of Engineering and Applied Science, California Institute of Technology, Pasadena, CA91125, USA. E-mail: jimbeck@caltech.edu

This paper presents the application of a new reliability method, called Subset Simulation (Au 2001; Au and Beck 2001), to compute the small failure probabilities encountered in seismic risk analysis where earthquake ground motions are described by a stochastic time-history model. The first-passage failure of the interstory drift above a specified threshold is considered for a linear moment-resisting steel frame with different types of uncertainties considered in the stochastic ground motion model. Failure analysis is also carried out using results from Subset Simulation which yields information about the probable scenarios that may occur in case of failure.

BASIC IDEA OF SUBSET SIMULATION

Given a failure region F, let $F_1 \supset F_2 \supset \cdots \supset F_m = F$ be a decreasing sequence of failure regions so that $F_k = \cap_{i=1}^{k} F_i$, $k = 1, \ldots, m$. For convenience, we denote the failure event by its corresponding failure region, then by the definition of conditional probability,

$$
\begin{aligned}
P(F) = P(F_m) = P(\cap_{i=1}^{m} F_i) &= P(F_m | \cap_{i=1}^{m-1} F_i) P(\cap_{i=1}^{m-1} F_i) \\
&= P(F_m|F_{m-1}) P(\cap_{i=1}^{m-1} F_i) = \cdots = P(F_1) \prod_{i=1}^{m-1} P(F_{i+1}|F_i)
\end{aligned}
\tag{2}
$$

Equation (2) expresses the failure probability as a product of a sequence of conditional probabilities $\{P(F_{i+1}|F_i) : i = 1, \ldots, m-1\}$ and $P(F_1)$. The idea of Subset Simulation is to estimate the failure probability $P(F)$ by estimating these quantities. In particular, standard Monte Carlo simulation is used to estimate $P(F_1)$. Estimating the conditional probabilities $P(F_{i+1}|F_i)$ ($i = 1, \ldots, m-1$) by simulation necessitates the efficient simulation of conditional samples distributed according to the conditional PDF $q(\underline{\theta}|F_i) = q(\underline{\theta})\, \mathbb{I}_{F_i}(\underline{\theta})/P(F_i)$. This is in general a non-trivial task. Nevertheless, it is accomplished by Markov Chain Monte Carlo Simulation (Fishman 1996), where the conditional samples are simulated as the states of a special Markov chain with a limiting stationary PDF equal to the conditional PDF. In spite of the fact that the samples are generally dependent, they can be used for statistical averaging to yield consistent estimates of conditional failure probabilities.

SUBSET SIMULATION PROCEDURE

The Subset Simulation procedure is outlined below. Details can be found in Au and Beck (2001) or Au (2001). First, we simulate N samples $\{\underline{\theta}_1, \ldots, \underline{\theta}_N\}$ by standard Monte Carlo simulation to compute an estimate $\tilde{P}_1$ for $P(F_1)$ by

$$
P(F_1) \approx \tilde{P}_1 = \frac{1}{N} \sum_{k=1}^{N} \mathbb{I}_{F_1}(\underline{\theta}_k) \tag{3}
$$

where $\{\underline{\theta}_k : k = 1, \ldots, N\}$ are independent and identically distributed (i.i.d.) samples simulated according to the parameter PDF q. From these samples, one readily obtains samples distributed as $q(\cdot|F_1)$, simply as those which lie in F_1. Starting from each of these samples, Markov chain Monte Carlo simulation is used to simulate additional samples which are also distributed as $q(\cdot|F_1)$. They can be used to estimate $P(F_2|F_1)$ using an estimator $\tilde{P}_2$ similar to (3). Those samples which lie in F_2 are distributed as $q(\cdot|F_2)$ and provide 'seeds' for simulating more samples according to $q(\cdot|F_2)$ to estimate $P(F_3|F_2)$. Repeating this process, one can compute the conditional probabilities of the higher conditional levels until the failure event of interest, F $(= F_m)$, has been reached. At the i-th conditional level, $1 \leq i \leq m-1$, let

$\{\underline{\theta}_{i,k} : k = 1, \ldots, N\}$ be the Markov chain samples with distribution $q(\cdot|F_i)$, possibly coming from different chains generated by different 'seeds.' Then

$$P(F_{i+1}|F_i) \approx \tilde{P}_{i+1} = \frac{1}{N} \sum_{k=1}^{N} \mathbb{I}_{F_{i+1}}(\underline{\theta}_{i,k}) \tag{4}$$

Finally, combining (2), (3) and (4), the failure probability estimator is $\tilde{P}_F = \prod_{i=1}^{m} \tilde{P}_i$. It can be shown that $\tilde{P}_F$ is asymptotically unbiased and its variance decays with $1/N$ as in standard Monte Carlo simulation (Au and Beck 2001).

FAILURE ANALYSIS USING MARKOV CHAIN SAMPLES

The Markov chain samples generated during Subset Simulation are used for estimating the conditional probabilities. Due to their conditional nature, they can also be used to infer the probable scenarios that may occur in case of failure. The distribution of some response quantity of interest, $h(\underline{\theta})$, evaluated at the Markov chain samples gives information about the system performance when failure occurs. In particular, using the Markov chain samples $\{\underline{\theta}_{i,k} : k = 1, \ldots, N\}$ conditional on the failure event F_i ($i = 1, \ldots, m$), the conditional expectation of $h(\underline{\theta})$ when the failure event F_i has occurred can be estimated by:

$$\mathsf{E}[h(\underline{\theta})|F_i] = \int h(\underline{\theta})\, q(\underline{\theta}|F_i)\, d\underline{\theta} \approx \frac{1}{N} \sum_{k=1}^{N} h(\underline{\theta}_{i,k}) \tag{5}$$

APPLICATIONS TO SEISMIC RISK BASED ON DYNAMIC ANALYSIS

Stochastic ground motion model

The seismic risk problem is formulated using a stochastic ground motion model to describe the uncertainty associated with the ground motion at the site in a seismic event of given magnitude and earthquake source location. The stochastic ground motion model developed by Atkinson and Silva (2000) (referred as the A-S model here) is adopted, which is a point-source model characterized by the moment magnitude M and epicentral distance r (Boore 1983). The model is characterized by the 'radiation spectrum' $A(f; M, r)$ and the 'envelope function' $e(t; M, r)$. To generate a time history for the ground acceleration for given M and r, a discrete-time white noise sequence $\{W_j = \sqrt{2\pi/\Delta t}\, Z_j : j = 1, \ldots, n_t\}$ is first generated, where $Z_1, \ldots, Z_{n_t}$ are i.i.d. standard Normal variables. The white noise sequence is then modulated by the envelope function $e(t; M, r)$ at the discrete time instants and the discrete Fourier transform is applied to the modulated white noise sequence. The resulting spectrum is multiplied with the radiation spectrum $A(f; M, r)$, after which the discrete inverse Fourier transform is applied to transform the sequence back to the time domain to yield a sample for the ground acceleration time history. The synthetic ground motion $a(t; \underline{Z}, M, r)$ is thus a function of the 'additive excitation parameters' $\underline{Z} = [Z_1, \ldots, Z_{n_t}]$ and the 'stochastic excitation model parameters' M and r.

Radiation Spectrum

The radiation spectrum consists of several factors which account for the spectral effects from the source and propagation through the Earth's crust. Figure 1 shows the radiation spectrum for $r = 20$ km, where the choice of the other model parameters used can be found in Au (2001). It can be seen that as the moment magnitude increases, the spectral amplitude increases at all frequencies, with a shift of dominant frequency content towards the lower frequency regime, as expected. Roughly speaking, both M and r have a multiplicative effect on the synthetic ground acceleration $a(t; \underline{Z}, M, r)$ and hence on the structural response.

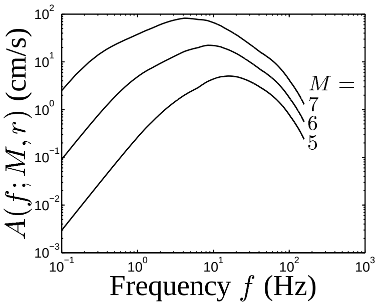

FIG. 1. Radiation spectrum $A(f;M,r)$ for $r = 20$ km, $M = 5, 6, 7$

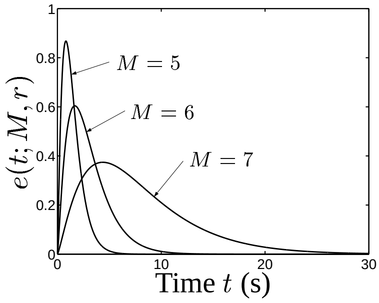

FIG. 2. Envelope function $e(t;M,r)$ for $r = 20$ km, $M = 5, 6, 7$

Envelope function

The envelope function is the major factor affecting the duration of simulated ground motions for given M and r. It is assumed to be

$$e(t;M,r) = c_3\, t^{c_1}\, \exp(-c_2\, t)\, U(t) \tag{6}$$

where $U(t)$ is the unit-step function, $c_1 = -\varepsilon_1 \log \varepsilon_2 / [1 + \varepsilon_1 (\log \varepsilon_1 - 1)]$, $c_2 = c_1/\varepsilon_1 T_w$ and $c_3 = \sqrt{(2c_2)^{2c_1+1}/\Gamma(2c_1+1)}$ is a normalizing factor such that the envelope function has unit energy, in the sense that $\int_0^\infty e(t;M,r)^2 dt = 1$. Here, $\Gamma(\cdot)$ is the Gamma function, and $T_w = 1/f_a + 0.1R$ is related to the duration of the envelope function. The parameters ε_1 and ε_2 are taken to be $\varepsilon_1 = 0.2$ and $\varepsilon_2 = 0.05$ (Boore 1983). The envelope function is shown in Figure 2 for $r = 20$ km. It can be seen that increasing the moment magnitude increases the duration of the envelope function, as expected.

Distribution of stochastic excitation model parameters

Using the A-S model, a synthetic ground acceleration $a(t;\underline{Z},M,r)$ for given M and r can be generated, where $\underline{Z} = [Z_1, \ldots, Z_{n_t}]$ is a standard Normal vector. When the seismic hazard aspect is to be addressed, the uncertainty in M and r has to be considered. The uncertainty in the moment magnitude is modeled by the Gutenberg-Richter relationship, i.e., an exponential distribution (with parameter chosen to be 2.3) truncated on the interval $[5, 8]$ (Gutenberg and Richter 1958). For the illustrative example considered here, earthquakes of magnitude between 5 and 8 are assumed to occur equally likely in a circular area of radius $r_{max} = 50$ km centered at the site where the structure is situated. This leads to a triangular distribution for r confined to the interval $[0, r_{max}]$. Also, M and r are modeled as stochastically independent.

Structure

A six-story moment-resisting steel frame (Figure 3) subjected to uncertain ground motions modeled by the A-S model is studied to illustrate the application of Subset Simulation to seismic risk analysis. It is modeled as a two-dimensional linear frame. Details of the structure can be found in Au (2001). The natural frequencies of the first two modes are 0.55 Hz and 1.56 Hz, respectively. Rayleigh damping is assumed so that the first two modes have 5% of critical damping. Failure is defined as the exceedence of a specified interstory drift ratio b at any one of the (twenty four) columns within the duration of interest. The sampling time and duration of study are taken to be 0.02 sec and 30 sec, respectively, for both the simulation of ground motions and dynamic structural analysis. The number of additive excitation parameters $\underline{Z}$ involved in the generation of ground motion for a given stochastic model is thus $n_t = 30/0.02 + 1 = 1501$, where the time instants at $t = 0$ and $t = 30$ are also represented.

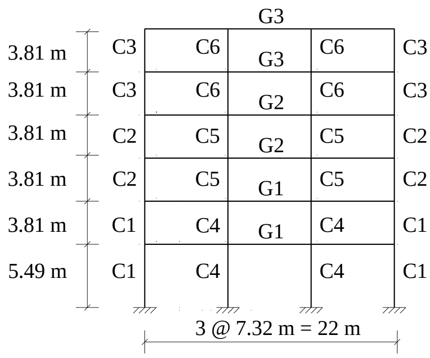

FIG. 3. Moment-resisting frame structure

Results

Two cases corresponding to different uncertain situations are considered. In Case 1, only the additive excitation parameters $\underline{Z}$ for generating the ground motion $a(t; \underline{Z}, M, r)$ are assumed to be uncertain; the moment magnitude M and epicentral distance r are fixed at the values: $M = 7$ and $r = 20$ km. This case corresponds to the classical first-excursion problem with a given stochastic excitation model defined by fixed M and r. In Case 2, in addition to the additive excitations, M and r are also considered to be uncertain, with the probability distributions described earlier. This corresponds to a seismic risk problem where the uncertainty in the regional seismicity is also addressed.

Note that by varying the threshold b, one can generate the complement of the cumulative distribution function for the peak interstory drift ratio. From this distribution, one can readily generate the corresponding distribution for the peak lifetime interstory drift ratio, e.g., if a Poisson model is used for the uncertain temporal occurrence of earthquakes in the region.

In the application of Subset Simulation, the conditional failure regions F_i are defined by the interstory drift ratio exceeding $b_i (i = 1, 2, 3)$ where these thresholds are adaptively chosen such that a conditional failure probability of $\tilde{P}_i = 0.1$ is attained. At each simulation level i, $N = 500$ samples are simulated with 50 samples from one level used to 'seed' the next level.

Failure probability estimation

Figures 4 and 5 show the estimates of failure probability for different threshold levels b for Cases 1 and 2, respectively. A total of $N_T = 1400$ samples, i.e., dynamic structural analyses, are performed to compute the results (solid line) in each figure. The results computed by standard Monte Carlo simulation (MCS) with $10,000$ samples are also shown for comparison. These figures show that the results computed using Subset Simulation give a good approximation to the failure probabilities. Further results not presented here confirm that Subset Simulation yields practically unbiased estimates and can lead to a substantial improvement in efficiency over standard Monte Carlo simulation, especially when estimating small failure probabilities.

Failure analysis using conditional samples

The Markov chain samples at the different failure levels simulated in a single run of Subset Simulation are next examined for the purpose of failure analysis. Figure 6 shows the typical samples of ground acceleration $a(t; \underline{Z}, M, r)$ that correspond to failure probabilities $10^{-1}, 10^{-2}$ and 10^{-3} (failure levels 1, 2 and 3, respectively) for Case 1. Note that only the additive excitation parameters $\underline{Z}$ are uncertain in this case. Since samples of acceleration time histories are generated for given moment magnitude $M = 7$ and epicentral distance $r = 20$ km,

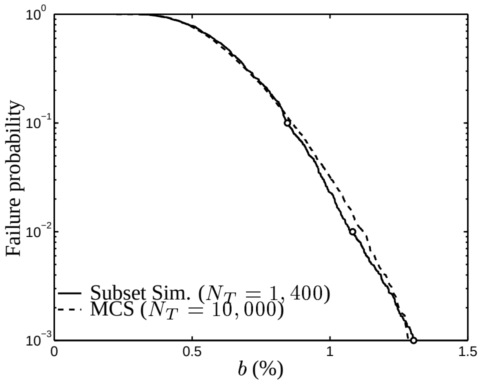

FIG. 4. Failure probability estimates for Case 1

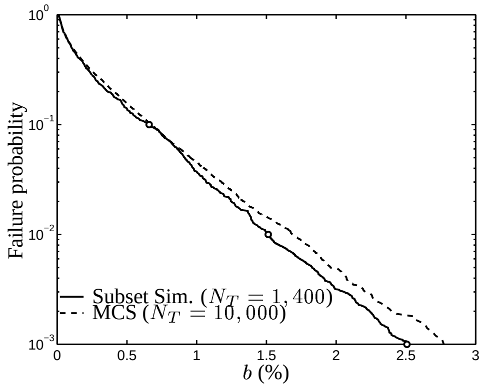

FIG. 5. Failure probability estimates for Case 2

there is not much difference in their duration as well as mean square values. In terms of peak acceleration, they do not differ significantly, either.

The major difference among the samples of ground acceleration that lead to different levels of failure lies in the frequency content. Figure 8 shows the average spectrum (power spectral density) of the additive excitation parameters $\underline{Z}$ corresponding to the 500 samples of acceleration time histories at different levels of failure. Level 0 refers to the initial phase of Subset Simulation where samples are generated directly from their parameter PDF, i.e., standard Monte Carlo simulation. The spectrum at Level 0 (top plot of Figure 8) is almost flat, because there is no conditioning on the samples at this level and therefore the spectrum theoretically corresponds to that of white noise, which is flat up to the Nyquist frequency, being $1/2\Delta t = 25$ Hz. As the simulation level increases, the spectrum develops a peak near 0.55 Hz, which is the fundamental frequency of the structure. This illustrates an important statistical feature of the additive excitations that lead to failure in the classical first-excursion problem (with deterministic structure and stochastic excitation model): *the additive excitation tends to 'tune' itself to the natural frequency of the structure to cause first-excursion failure.* In other words, when the stochastic excitation model parameters are fixed, the probable cause of failure for the structure is due to resonance effects, especially when the threshold level is high. This phenomenon can be explained from the high dimensional features of the reliability problem (Au 2001).

The situation is different when the stochastic excitation model parameters, M and r, are also uncertain. Figures 7 and 9 show the conditional samples and the average spectra at different simulation levels for Case 2, where $\underline{Z}$, M and r are considered uncertain in the problem. Figure 7 shows that in this case the excitation intensity and duration of the ground acceleration differ significantly at different simulation levels. Both the excitation intensity and duration increase as the simulation level increases. From Figure 9, it can be seen that the spectral peak at 0.55 Hz for Levels 2 and 3 is not as significant as observed in Case 1 (Figure 8). This indicates that the frequency content of the additive excitation $\underline{Z}$ when failure occurs is not significantly different from its original spectrum (flat), although this does not imply that the frequency content of the ground acceleration will be the same irrespective of whether failure occurs, since the radiation spectrum $A(f; M, r)$ could be different because of the change in the distribution of M and r when failure occurs.

When the moment magnitude M and the epicentral distance r are uncertain (Case 2), they are the parameters that control failure. Figure 10 shows the scattering of samples of (M, r) at different simulation levels. Note that the samples of (M, r) at Level 0 are simulated according

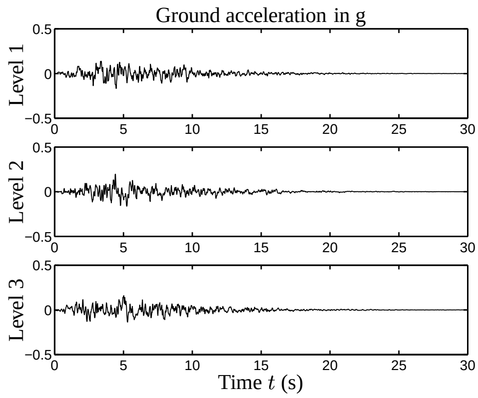

FIG. 6. Ground motions for Case 1, conditional levels 1, 2, 3

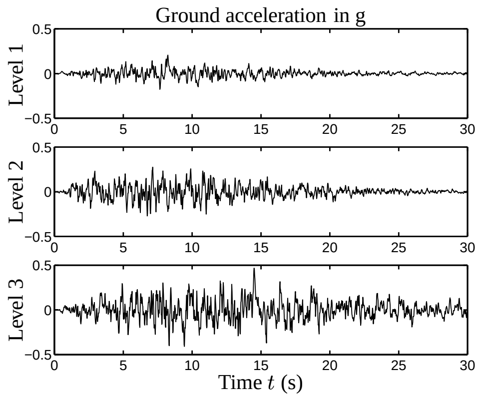

FIG. 7. Ground motions for Case 2, conditional levels 1, 2, 3

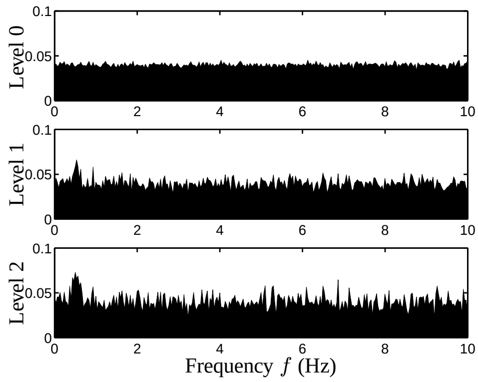

FIG. 8. Spectra of $\underline{Z}$ for Case 1, conditional levels 0, 1, 2

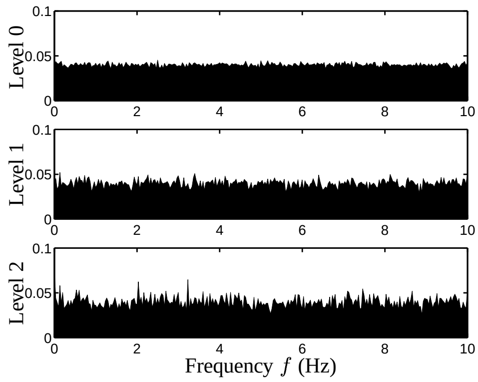

FIG. 9. Spectra of $\underline{Z}$ for Case 2, conditional levels 0, 1, 2

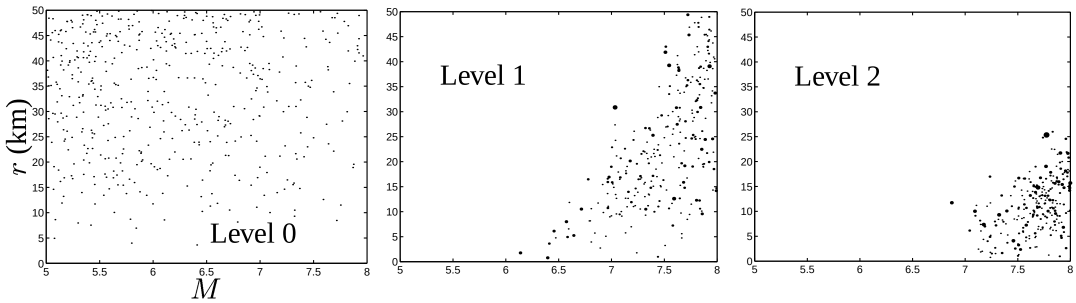

FIG. 10. Conditional samples of (M, r) for Case 2 at conditional levels 0, 1, 2

to their joint PDF. Also, for Levels 1 and 2, some of the locations shown in the figure contain repeated samples. Since the Markov chain samples are not all distinct, to show the population of the samples consistently, the dots are shown with area proportional to the number of points situated at the particular location. Figure 10 clearly indicates that as the simulation level increases, that is, when failure becomes more severe, the samples of (M, r) shift towards the 'large magnitude, small distance' regime.

CONCLUSIONS

Subset Simulation has been applied to compute the failure probabilities of structures during seismic risk studies using dynamic analysis. Failure analysis has been carried out using the samples generated during Subset Simulation to gain insight into the system behavior when failure occurs. This analysis shows that when only the seismic ground acceleration time history is uncertain, the rare failure scenarios correspond to resonance of the excitation with the structure. On the other hand, when the earthquake magnitude M and epicentral distance r defining the stochastic excitation model are also uncertain, they tend to control failure, due to their multiplicative effects on the response. The conditional joint distribution of M and r given that failure occurs is significantly different from their original joint PDF.

It should be noted that the observations from the failure analysis, such as the distribution of the moment magnitudes and epicentral distance when failure occurs, are based on the assumed probability models for the ground acceleration. The results should be interpreted bearing in mind the inherent limitations of these models. For example, the Atkinson-Silva model is a point-source model which does not directly account for the geometry of the fault and the characteristics of near-source ground motions. In view of this, the failure analysis results either provide a means for calibrating the stochastic ground motion models, or otherwise should be interpreted carefully. Nevertheless, on the premise that the quality of stochastic ground motion models will improve, Subset Simulation provides an efficient tool for estimation of failure probabilities and for failure analysis.

ACKNOWLEDGEMENT

This paper is based upon work partly supported by the Pacific Earthquake Engineering Research Center under National Science Foundation Cooperative Agreement No. CMS-9701568. This support is gratefully acknowledged. Part of this work was prepared when the first author was at graduate standing at the California Institute of Technology, whose generous financial support is gratefully acknowledged.

REFERENCES

Atkinson, G. M. and Silva, W. (2000). “Stochastic modeling of California ground motions.” *Bulletin of the Seismological Society of America*, 90(2), 255–274.

Au, S. K. (2001). “On the solution of first excursion problems by simulation with applications to probabilistic seismic performance assessment.” *PhD Thesis in Civil Engineering, EERL Report No. 2001-02*, California Institute of Technology, Pasadena. Available at URL `http://www.ntu.edu.sg/home/cskau`.

Au, S. K. and Beck, J. L. (2001). “Estimation of small failure probabilities in high dimensions by subset simulation.” *Probabilistic Engineering Mechanics*, 16(4), 263–277.

Boore, D. M. (1983). “Stochastic simulation of high-frequency ground motions based on seismological models of the radiated spectra.” *Bulletin of the Seismological Society of America*, 73(6), 1865–1894.

Engelund, S. and Rackwitz, R. (1993). “A benchmark study on importance sampling techniques in structural reliability.” *Structural Safety*, 12, 255–276.

Fishman, G. S. (1996). *Monte Carlo: Concepts, Algorithms, and Applications*. Springer-Verlag, New York.

Gutenberg, B. and Richter, C. (1958). “Earthquake magnitude, intensity and acceleration.” *Bulletin of the Seismological Society of America*, 62(2), 105–145.

Schuëller, G. I., Pradlwarter, H. J., and Pandey, M. D. (1993). “Methods for reliability assessment of nonlinear systems under stochastic dynamic loading – a review..” *Proceedings of EURODYN’93*. Balkema, 751–759.